Rigor-Force Producing Cross-Bridges in Skeletal Muscle Fibers Activated by a Substoichiometric Amount of ATP

Takenori Yamada,* Yasunori Takezawa,† Hiroyuki Iwamoto,* Suechika Suzuki,* and Katsuzo Wakabayashi†
*Department of Physiology, School of Medicine, Teikyo University, Tokyo 173-8605, Japan; and †Division of Biophysical Engineering, Graduate School of Engineering Science, Osaka University, Toyonaka, Osaka 560-8531, Japan

ABSTRACT Isometric skinned muscle fibers were activated by the photogeneration of a substoichiometric amount of ATP and their cross-bridge configurations examined during the development of the rigor force by x-ray diffraction and electron microscopy. By the photogeneration of ~100 μM ATP, ~2/3 of the concentration of the myosin heads in a muscle fiber, muscle fibers originally in the rigor state showed a transient drop of the force and then produced a long-lasting rigor force (~50% of the maximal active force), which gradually recovered to the original force level with a time constant of ~4 s. Associated with the photoactivation, muscle fibers revealed small but distinct changes in the equatorial x-ray diffraction that run ahead of the development of force. After reaching a plateau of force, long-lasting intensity changes in the x-ray diffraction pattern developed in parallel with the force decline. Two-dimensional x-ray diffraction patterns and electron micrographs of the sectioned muscle fibers taken during the period of 1–1.9 s after the photoactivation were basically similar to those from rigor preparations but also contained features characteristic of fully activated fibers. In photoactivated muscle fibers, some cross-bridges bound photogenerated ATP and underwent an ATP hydrolysis cycle whereas a significant population of the cross-bridges remained attached to the thin actin filaments with no available ATP to bind. Analysis of the results obtained indicates that, during the ATP hydrolysis reaction, the cross-bridges detached from actin filaments and reattached either to the same original actin monomers or to neighboring actin monomers. The latter cross-bridges contribute to produce the rigor force by interacting with the actin filaments, first producing the active force and then being locked in a noncycling state(s), transforming their configuration on the actin filaments to stably sustain the produced force as a passive rigor force.

INTRODUCTION

The contraction of muscle fibers takes place by relative sliding motions between thin and thick filaments utilizing the chemical energy of ATP hydrolysis. The most popular model assumes that the force for the sliding motion is produced when the attached myosin heads alter their conformation over the thin actin filaments (Huxley, 1969).

To experimentally detect the configurational changes of a myosin cross-bridge responsible for the force production, extensive studies have been made on contracting muscle fibers (Irving et al., 1992; Hirose et al., 1993; Yagi et al., 1996; Allen et al., 1996; Lenart et al., 1996; Katayama, 1998; Dobbie et al., 1998; Corrie et al., 1999). On the other hand, x-ray solution scattering studies (Wakabayashi et al., 1992; Sugimoto et al., 1995; Mendelson et al., 1996), x-ray crystallographic studies (Fisher et al., 1995; Houdusse et al., 2000), and fluorescent energy transfer studies (Suzuki et al., 1998; Shih et al., 2000) of the myosin heads with various nucleotides have shown several distinct different conformations, implicating that the myosin heads change their conformation depending upon bound nucleotide. Analysis of x-ray solution scattering (Sugimoto et al., 1995; Mendelson et al., 1996) and spectroscopic data (Highsmith and Eden, 1993) of isolated myosin heads indicated that the long α-helical regulatory domain deformed globally relative to its catalytic domain during the ATPase cycle. The superposition of the atomic structure of the myosin head and the actin molecules elucidated by x-ray crystallography (Rayment et al., 1993a; Kabsch et al., 1990) upon the reconstructed image of the electron micrograph of the actin filament decorated with myosin heads suggested that the myosin heads could bind to the actin filaments and make a tilting motion over the actin filaments without steric hindrance (Rayment et al., 1993b; Taylor et al., 1999). Based on these studies, the ''lever-arm'' hypothesis has been proposed and discussed for the molecular mechanism of muscle contraction in which the intramolecular domains of the myosin head alter their configuration(s) in a lever-like fashion to generate the contractile force (Irving et al., 1992; Fisher et al., 1995; Yagi et al., 1996; Cooke, 1997; Dobbie et al., 1998; Corrie et al., 1999; Linari et al., 2000).

On the other hand, it is well known that muscle fibers produce a force (the so-called rigor force) at the terminal point of contractile activities. Although the rigor force is considered to be a passively produced force, it is generated after the active force production when cross-bridges hydro-

Submitted May 9, 2002, and accepted for publication April 10, 2003.

Address reprint requests to Dr. Takenori Yamada, Dept. of Physics (Biophysics Section), Faculty of Science, Tokyo University of Science, 1-3 Kagurazaka, Shinjuku-ku, Tokyo 162-8601, Japan. Tel.: 81-3-5228-8228; Fax: 81-3-5261-1023; E-mail: yamada@rs.kagu.tus.ac.jp.

Dr. T. Yamada's present address is Department of Physics (Biophysics Section), Faculty of Science, Tokyo University of Science, Shinjuku-ku, Tokyo 162-8601, Japan.

Dr. H. Iwamoto's present address is Japan Synchrotron Radiation Research Institute (SPring-8), Mikazuki, Sayo, Hyogo 679-5198, Japan.

Dr. S. Suzuki's present address is Department of Applied Biological Science, Faculty of Science, Kanagawa University, Hiratsuka, Kanagawa 259-1293, Japan.

0006-3495/03/09/1741/13 $2.00

lyzing the last stock of ATP finally attach to the thin actin filaments, forming rigor complexes. Therefore it could be argued whether the cross-bridges producing the rigor force are in the rigor configuration(s) or in the active force-generating configuration(s). As far as we know, however, no studies have been made on the configurational changes of cross-bridges associated with the production of rigor force in muscle fibers. In the present studies, therefore, the cross-bridge configurations in muscle fibers during the rigor force production were investigated by x-ray diffraction and electron microscopy. Such work will provide some help for understanding the force generation mechanism by acto-myosin cross-bridge interaction in actively contracting muscle. The rigor force can conventionally be produced in muscle fibers by immersing skinned relaxed fibers in bathing solutions containing no ATP (Kawai and Brandt, 1976). However, in such muscle fibers, the rigor force may be produced by cross-bridges with configurations broadly distributed over various intermediate states in the ATPase cycle. That will make the analysis of the results so obtained be complicated. Previously Yamada et al. (1993) reported that muscle fibers could synchronously be activated by the photolysis of caged ATP and that unloaded muscle fibers uniformly shortened the distances determined by the amount of photogenerated ATP. Here, under isometric conditions, we similarly photoactivated muscle fibers with a substoichiometric amount of ATP and examined their cross-bridge configurations during the development of the rigor force by x-ray diffraction using intense synchrotron radiation and quick-freeze electron microscopic techniques.

Preliminary results were published in an abstract form (Yamada et al., 1994a,b).

MATERIALS AND METHODS

Muscle fiber preparation

Muscle strips (~1 mm in diameter, 20–30 mm in length) were dissected from the psoas muscle of a New Zealand white rabbit stunned and killed by exsanguination. The muscle strips were fixed on a silicone-covered trough by pinning both ends of the fiber strips at slightly stretched lengths (~1.2 times slack length) and skinned in a relaxing solution (see Table 1 for composition) containing 0.5% Triton X-100 for 30 min at 0°C. Then the fiber strips were washed several times with a fresh relaxing solution. The bathing solution was exchanged with a 50% glycerol solution containing 50 mM K^+-propionate, 4 mM $MgCl_2$, 4 mM EGTA, 5 mM ATP, and 20 mM imidazole (pH 7.0) and kept in this solution at 0°C overnight. After an exchange of solution, the fiber strips were stored at −20°C for several weeks before use.

Experimental apparatus

A portable experimental assembly composed of compartments for mechanical measurements and for light-flash irradiation was built in-house (by H. Iwamoto). A muscle preparation was mounted in a mechanical compartment. It had a linear series of four chambers, each of which was filled with an appropriate solution (~0.1 ml in volume). By moving the chambers in vertical and horizontal directions by using a mechanical controller, the muscle preparation was immersed in a solution in one or another of the chambers. The fiber preparation could be lifted in air for exposure to UV light as well as x-ray irradiation. In a light-flash compartment, an Xe-flash lamp system (SA-200E, Eagle, Tokyo, Japan) produced light flashes (duration of 100 μs; wavelength, 300–400 nm; intensity, up to 100 mJ). The emitted light was collimated with an elliptical mirror and led through a liquid optical fiber to the muscle preparation mounted in the mechanical compartment. The emitted light beam had a circular cross section (~7 mm in diameter) with a uniform intensity over the entire spot area. This light-flash photolyzed caged ATP to release free ATP in the myofibrillar space.

Estimation of the amount of photogenerated ATP in muscle fibers

In all the following photoactivation experiments, a certain stoichiometric amount of free ATP, ~100 μM, was photogenerated in muscle fibers containing caged ATP by adjusting the intensity of light flashes illuminating the muscle fibers. The amount of ATP photogenerated from caged ATP in muscle preparations was estimated as described by Yamada et al. (1993). A caged-ATP solution (5 μl) containing 1 mM caged ATP was put into a small circular plastic trough (~4 mm in diameter) and it was placed in the mechanical compartment of the experimental assembly so that the entire surface of the solution was irradiated with the light flash at the same location where muscle fibers were mounted. The irradiated solutions were recovered from the trough, and applied to a high-performance liquid chromatography system (L-6200, Hitachi, Tokyo, Japan). The column (4.6 mm in diameter) packed with 5-μm beads was a C-18 type (ODS-H-1251, Senshu Scientific, Tokyo, Japan). An eluting solution contained 10 mM KH_2PO_4 (pH 5.5) and methanol (85:15 (v/v)), and the eluent was monitored at a wavelength of 260 nm. The amount of ATP photogenerated in the irradiated solutions was determined based on the peak area for ATP relative to that for caged ATP. The concentration of free ATP photogenerated in muscle preparations equilibrated with a caged-ATP solution was thus estimated to be 103 ± 5 μM (n = 25), which is about two-thirds of the concentration of myosin heads in a muscle fiber, 154 μM (Ferenczi et al., 1984).

TABLE 1 Compositions of experimental solutions

Solution	K^+-propionate	$MgCl_2$	$CaCl_2$	EGTA	Imidazole	ATP	Caged ATP	GSH*
Contracting solu.†	80	5	2	4	20	4	0	0
Relaxing solu.	80	5	0	10	20	4	0	0
Rigor solu.	80	5	0	4	20	0	0	0
Caged-ATP solu.	80	5	2.1	2	20	0	1	30

Concentration of each chemical is given in mM.

*GSH, glutathione (reduced form).

†This solution contained 20 mM of phosphocreatine and 125 units/ml of creatine kinase.

Force and stiffness measurements

A bundle composed of 5–7 single muscle fibers was carefully dissected from glycerinated muscle strips. Each end of the fiber bundle was clamped with an aluminum T-clip. The muscle fiber bundle (~2 mm in length) was mounted horizontally in the mechanical compartment of the above experimental assembly by fixing it between the extensions from a force transducer and from an actuator with the aluminum T-clips. The fiber bundle was immersed in a relaxing solution, and the sarcomere length was adjusted to 2.4–2.5 μm by the optical diffraction of a He-Ne laser light. To determine the maximum active force, the muscle fiber bundle was transferred to a contracting solution and the developed force was measured as below.

The force transducer was of a semiconductor type (AE801, SensoNor, Horten, Norway) (elastic modulus, 2 N/mm; resonance frequency, 2 kHz), and the actuator was a servomotor equipped with a controller (G100PD/JCCX-101, General Scanning, Watertown, MA USA). The sinusoidal voltages produced with a waveform generator (Type 1930, NF Electronic Instruments, Tokyo, Japan) were applied to the servomotor. The movement of the servomotor arm was detected by the use of a displacement transducer (differential-transformer type), which was incorporated into the servomotor. The stiffness of muscle fibers was estimated by continuously applying small sinusoidal length changes (0.3% muscle length, 1 kHz) to muscle fibers with the servomotor and measuring the amplitude of resulting force changes. The force and length changes of muscle fibers were simultaneously recorded on a digital oscilloscope (Model 3091, Nicolet, Madison, WI USA) and stored into the memory. The stored data were transferred into a computer (PC98RL, NEC, Tokyo, Japan) for processing and analysis.

Synchrotron x-ray diffraction measurements

X-ray diffraction experiments of muscle fibers using synchrotron radiation were made essentially as described by Wakabayashi and Amemiya (1991) and Takezawa et al. (1999). The x-ray source was a monochromatized beam (~0.5 mm (V) × 1.5 mm (H); wavelength of 0.15 nm) selected and collimated from synchrotron radiation emitted from the beam line 15A port of the positron storage ring at the Photon Factory, KEK (Tsukuba, Japan). After mounting a muscle fiber bundle in the mechanical compartment of the portable experimental assembly as described above, the whole experimental assembly was installed on the x-ray beam line. The position of the assembly was adjusted so that the x-ray beam hit the muscle preparation properly. The muscle preparations were exposed to x-rays by opening a mechanical shutter placed in front of the specimen. One-dimensional equatorial and two-dimensional x-ray diffraction patterns from muscle fibers were recorded respectively with a linear position-sensitive proportional detector (1D-PSD, Rigaku Denki, Tokyo, Japan) and a storage-phosphor area detector (an image plate, BAS-III type, Fuji Photo Film, Tokyo, Japan). The sample-to-detector distance was ~2.3 m for the equatorial diffraction measurements and ~1.3 m for the two-dimensional diffraction measurements. The force exerted by muscle fibers was continuously monitored on a computer display during x-ray experiments.

X-ray diffraction measurements of photoactivated muscle fibers were made under isometric conditions as follows. A muscle fiber bundle mounted as above was first immersed in a relaxing solution and then transferred into a rigor solution. After muscle fibers fully developed a rigor force, the muscle preparation was dipped in a caged-ATP solution for 30 s. Then it was lifted in air and irradiated with a light flash to generate ATP. Shortly after the light flash, it was immersed in the relaxing solution again. While the muscle preparation was lifted in air, it was exposed to x-ray beams for appropriate time periods to obtain x-ray diffraction data. The above procedure was repeated 3–4 times for each muscle preparation and all the data were accumulated. X-ray measurements were conducted for 6–7 separate muscle preparations, and the obtained data were summed up for the analysis.

X-ray diffraction measurements of relaxed muscle fibers were performed by lifting in air a muscle preparation dipped in a relaxing solution and exposing it to x-ray beams for 1 s. To obtain x-ray diffraction patterns of rigor muscle fibers, a muscle preparation in a relaxing solution was transferred into a rigor solution. After muscle fibers fully developed the rigor force, the muscle preparation was lifted in air and exposed to x-ray beams for 1 s. X-ray diffraction measurements of fully Ca^{2+}-activated muscle fibers under isometric conditions were similarly made after muscle preparations developed full force by dipping them into a contracting solution containing a backup system for ATP regeneration (see Table 1). In these experiments, x-ray diffraction measurements were made for 3–5 separate muscle preparations except for Ca^{2+}-activation, and the obtained data were accumulated for the analysis.

All x-ray diffraction measurements were performed at room temperature (22–24°C).

Measurement of intensity of x-ray reflections

The integrated intensities of the 1,0 and 1,1 equatorial reflections in the static x-ray diffraction patterns and in the time-resolved x-ray diffraction patterns with 256 time frames taken with the 1D-PSD were obtained by integrating the areas under the reflection peaks. The background under each peak was drawn by a second-order polynomial fit. The intensities of these reflections were adopted as the mean value of those on the left and right sides of the diffraction pattern.

The intensity data from the image plates were digitally read out with an image reader (BAS 2000 scanner, Fuji Photo Film) and analyzed as detailed by Takezawa et al. (1999). The four quadrants of the x-ray diffraction images were folded and averaged. The intensity distributions of the layer-line reflections were measured by scanning the data along rows of pixels perpendicular to the layer lines and expressed as a function of the reciprocal radial coordinate (R). The integrated intensity of each peak on the layer-line reflections was obtained by integrating the intensities of the peak over a polynomial background line that was drawn by smoothly connecting the data points of each side of the peak in the axial direction. For the 7.1-nm and 36.7-nm actin-based layer lines, the intensities were integrated in the radial range of $0.030 < R < 0.136$ nm^{-1}, and for the 5.1-nm and 5.9-nm actin-based layer lines, the intensities were integrated in the range of $0 < R < 0.130$ nm^{-1} and $0 < R < 0.142$ nm^{-1}, respectively. For the 2.7-nm actin-based meridional reflection, the intensity was integrated in the range of $0 < R < 0.130$ nm^{-1}. For the 14.4-nm and 7.2-nm myosin-based meridional reflections, the intensities were integrated in the range of $0 < R < 0.035$ nm^{-1} and $0 < R < 0.059$ nm^{-1}, respectively.

Axial spacing measurements were made as follows (for detail, see Wakabayashi et al. (1994) and Takezawa et al. (1999)). For the 5.1-nm and 5.9-nm layer lines, the intensities were integrated in the radial range of $0 < R < 0.094$ nm^{-1}, and for the 2.7-nm meridional reflection and the 14.4-nm myosin-based meridional reflections, the intensities were integrated in the range of $0 < R < 0.030$ nm^{-1}. They were traced along the axial direction. The centroid of each axial reflection profile was determined by assuming a Gaussian model for the peak over a polynomial background.

Quick-freeze electron microscopy

For quick-freeze electron microscopic observations of muscle fibers, muscle preparations were frozen and treated as described by Suzuki and Sugi (1983) and Suzuki et al. (1993). A muscle preparation was mounted under isometric conditions in a mechanical apparatus having long beams (~30 mm in length) extending from the force transducer and from the actuator and it was photoactivated as for the x-ray diffraction measurements. The force exerted by muscle fibers was continuously monitored during the freezing procedure. Photoactivated muscle fibers were frozen by quickly dipping a muscle fiber preparation into preevacuated liquid N_2 at an appropriate time after an Xe-light flash illumination of muscle fibers equilibrated with a caged-ATP solution. Rigor muscle fibers were similarly frozen by quickly dipping a muscle fiber preparation into preevacuated liquid N_2 when the muscle preparation fully developed the rigor force after transferring it from

a relaxing solution into a rigor solution. Frozen muscle fibers were freeze-substituted with 2% OsO_4 in acetone at −80°C for two days, warmed to −20°C, transferred into fresh OsO_4/acetone, and kept in it for ~2 h. Then they were warmed gradually to room temperature, rinsed with acetone, and stained en bloc with uranyl acetate. They were rinsed with a series of increased concentrations of ethanol to get dehydrated. The dehydrated samples were embedded in Epon 812 resin and sliced into ultrathin sections (~30 nm in thickness) with a Porter-Blum ultramicrotome (DEMT-2, DuPont Instruments Sorvell, DuPont, Wilmington, DE USA). The thin sections of muscle fibers were doubly stained with uranyl acetate and lead citrate and examined with a transmission electron microscope (JEM 100CX, JOEL, Tokyo, Japan).

Analysis of cross-bridge angles in electron micrographs

The myosin cross-bridge angle to the thick filament axis in the electron micrographs of sectioned muscle fibers was determined by the use of a digital image processor (Tospix II, Toshiba, Tokyo, Japan) as detailed by Suzuki et al. (1993). In the electron micrographs (~300,000× in magnification) of muscle preparations cut along the (110) lattice plane of a hexagonal myofilament array, the overlap regions of thick and thin filaments were first processed to produce contour images of filaments and cross-bridges. The contour images were converted into short-rod images running through the center of the contours. By referring to the original electron micrographs, the rod images representing cross-bridges, thick filaments, and thin filaments were specified by eye. Finally the cross-bridge angle to the thick filament axis was determined by measuring the angle of the rod images from cross-bridges to those from thick filaments.

Optical diffraction patterns of a He-Ne laser light from the negative electron micrographs of sectioned muscle fibers were obtained by the use of an optical diffractometer (Sigma-Koki, Saitama, Japan).

Solutions

Composition of bathing solutions used in the experiments is listed in Table 1. The pH of each solution was adjusted to 7.0. ATP and glutathione (GSH, reduced form) were purchased from Sigma Chemical (St. Louis, MO). Caged ATP of highly purified grade was purchased from Dojindo Laboratories (Kumamoto, Japan) and used without further purification. All other chemicals were of analytical grade and purchased from Wako Pure Chemical (Osaka, Japan).

RESULTS

Force production in photoactivated muscle fibers

The isometric force production of muscle fibers was examined when ~100 μM ATP was photogenerated in rabbit psoas muscle fibers. A bundle of skinned single muscle fibers was mounted in the experimental apparatus, and immersed in a relaxing solution under isometric conditions. When the fiber bundle was transferred into a rigor solution, muscle fibers developed a force, the so-called rigor force (cf. Fig. 1 *A*). When muscle fibers fully exerted the rigor force, the muscle preparation was transferred into a caged-ATP solution. After muscle fibers were equilibrated with caged ATP, the muscle preparation was lifted in air and illuminated with an Xe-light flash so as to produce ATP.

After the photoactivation, muscle fibers developed a long-lasting rigor force, in the early plateau phase of which the force level increased by ~60% over the original rigor force to ~50% of the maximal active force in magnitude separately measured. The produced rigor force eventually declined very gradually to the original force level with a time constant of ~4 s (e.g., see Fig. 2 *B*). Then the muscle fibers were put into the relaxing solution, which caused the force level to quickly drop to naught. In some experiments, the changes of the stiffness of muscle fibers were simultaneously examined during the force measurements. In the enlarged traces of the force and stiffness changes shown in Fig. 1 *B*, muscle fibers transiently caused a small decrease in the force level immediately after the photoactivation and then developed a stable force with a half-time of ~55 ms. The stiffness of muscle fibers transiently decreased by ~25% in ~70 ms after the photoactivation and quickly returned to the original level as the force developed. Muscle fibers immersed in a caged-ATP solution were in the rigor state before illumination of the light flash, as the stiffness of muscle fibers in this solution was comparable in magnitude to that of rigor muscle fibers, and muscle fibers did not shorten at all in this solution (Yamada et al., 1993).

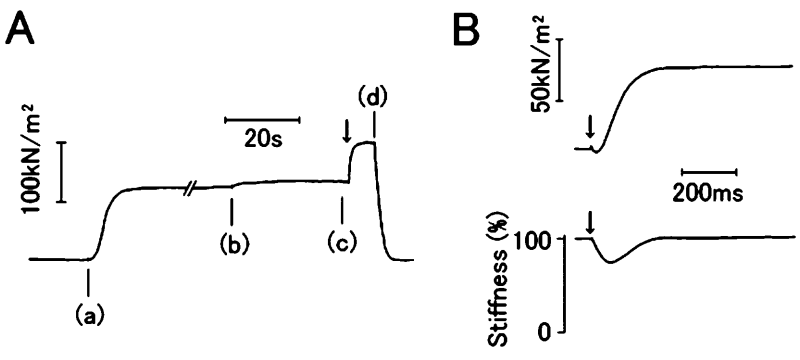

FIGURE 1 (*A*) Force trace showing how a bundle of glycerinated single muscle fibers was activated by the photogeneration of a substoichiometric amount of ATP. A muscle preparation, immersed in a relaxing solution, was transferred into a rigor solution at *a*. After the muscle preparation developed the so-called rigor force, it was transferred into a caged-ATP solution at *b*. After incubating to equilibrate caged ATP in muscle fibers, the muscle preparation was lifted in air at *c* and irradiated with a light flash to produce ~100 μM ATP by the photolysis of caged ATP at the time indicated by an arrow. Then the muscle preparation was immersed in the relaxing solution at *d*. (*B*) Enlarged force (*upper*) and stiffness (*lower*) traces of the muscle preparation during the photoactivation. At the time indicated by an arrow, the muscle preparation was photoactivated.

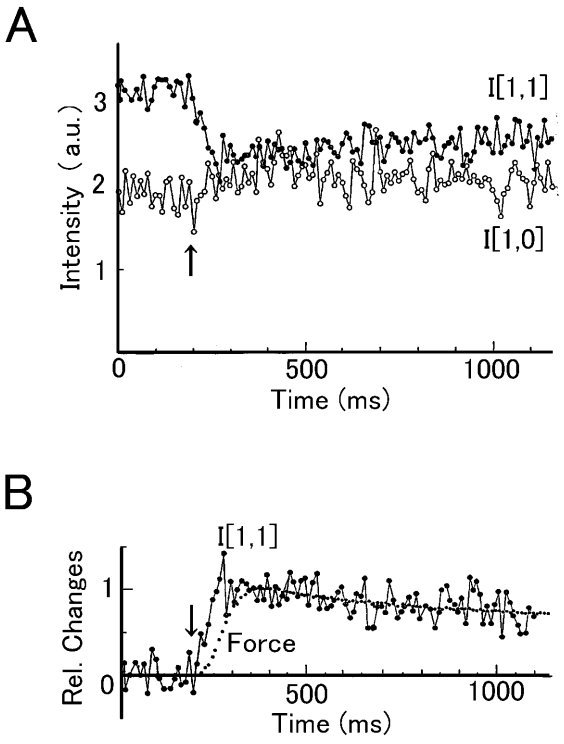

FIGURE 2 (*A*) Time-resolved intensity changes of the 1,0 and 1,1 x-ray equatorial reflections taken in a time resolution of 5 ms upon the photoactivation of rigor muscle fibers. The 1,0 reflection (○) and the 1,1 reflection (●). (*B*) Comparison between the time-dependent changes of the 1,1 reflection intensity and the force development of muscle fibers. The 1,1 reflection (●), and the dotted curve, the force development. The two curves were normalized in the time range of 350–500 ms based on the least mean-square fit. In *A* and *B*, the muscle preparations were photoactivated at the time indicated by an arrow.

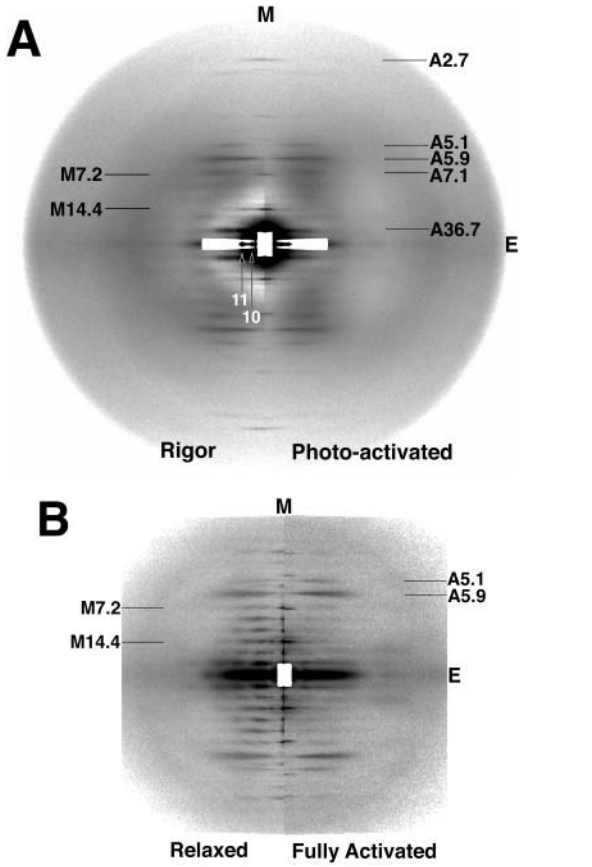

FIGURE 3 Two-dimensional x-ray diffraction patterns from muscle fibers in the rigor, photoactivated, relaxed, and fully activated states. (*A*) The left- and right-half patterns are from rigor muscle fibers before the photoactivation and from photoactivated muscle fibers, respectively. (*B*) The left- and right-half patterns are from relaxed fibers and from fully Ca^{2+}-activated fibers, respectively. The fiber axis of the muscle is in vertical direction. M, the meridional axis; E, the equatorial axis. The two arrows with 10 and 11 in *A* indicate the 1,0 and 1,1 equatorial reflections, respectively. M7.2 and M14.4 represent the 7.2-nm and 14.4-nm myosin-based second and first order reflections with a 14.4-nm repeat, respectively. A2.7, A5.1, A5.9, A7.1, and A36.7 represent the 2.7-nm, 5.1-nm, 5.9-nm, 7.1-nm, and 36.7-nm actin-based reflections, respectively.

X-ray diffraction patterns from photoactivated muscle fibers

First, the changes of the equatorial x-ray diffraction produced by the photogeneration of ~100 μM ATP in rigor muscle fibers were measured with the 1D-PSD. The static pattern obtained from photoactivated muscle fibers and that from rigor muscle fibers before the photoactivation were very similar (data not shown) but there were small but significant differences in the strongest 1,0 and 1,1 reflections coming respectively from the (100) and (110) lattice planes of the hexagonal myofilament array (see Fig. 3 *A*). Thus the time-dependent intensity changes of both reflections upon the photoactivation were measured in a time-resolution of 5 ms. As shown in Fig. 2 *A*, after the photoactivation, the intensity of the 1,0 reflection increased by ~15% whereas that of the 1,1 reflection decreased by ~25%, both having a half-time of 50–70 ms. After reaching their maximum changes, both intensities gradually recovered to their original values. In Fig. 2 *B*, the time course of the 1,1 intensity change is compared with that of the development of force. The intensity change preceded the force development by ~50 ms at their half maximal changes, and after reaching the peak the intensity gradually decreased almost in parallel to the decline of the rigor force.

Next, two-dimensional x-ray diffraction patterns from photoactivated muscle fibers were examined. They were taken with the area detector (the image plate) at a shorter camera length during the period of 1.0–1.5 s after the photoactivation. Fig. 3 *A* shows a comparison of the x-ray diffraction pattern from photoactivated muscle fibers (*right half*) and that from rigor muscle fibers before the photoactivation (*left half*). For reference, in the left and right halves of Fig. 3 *B* are shown the x-ray diffraction patterns from relaxed and fully Ca^{2+}-activated muscle fibers, respectively. All these x-ray diffraction patterns were taken under the same conditions. It can clearly be

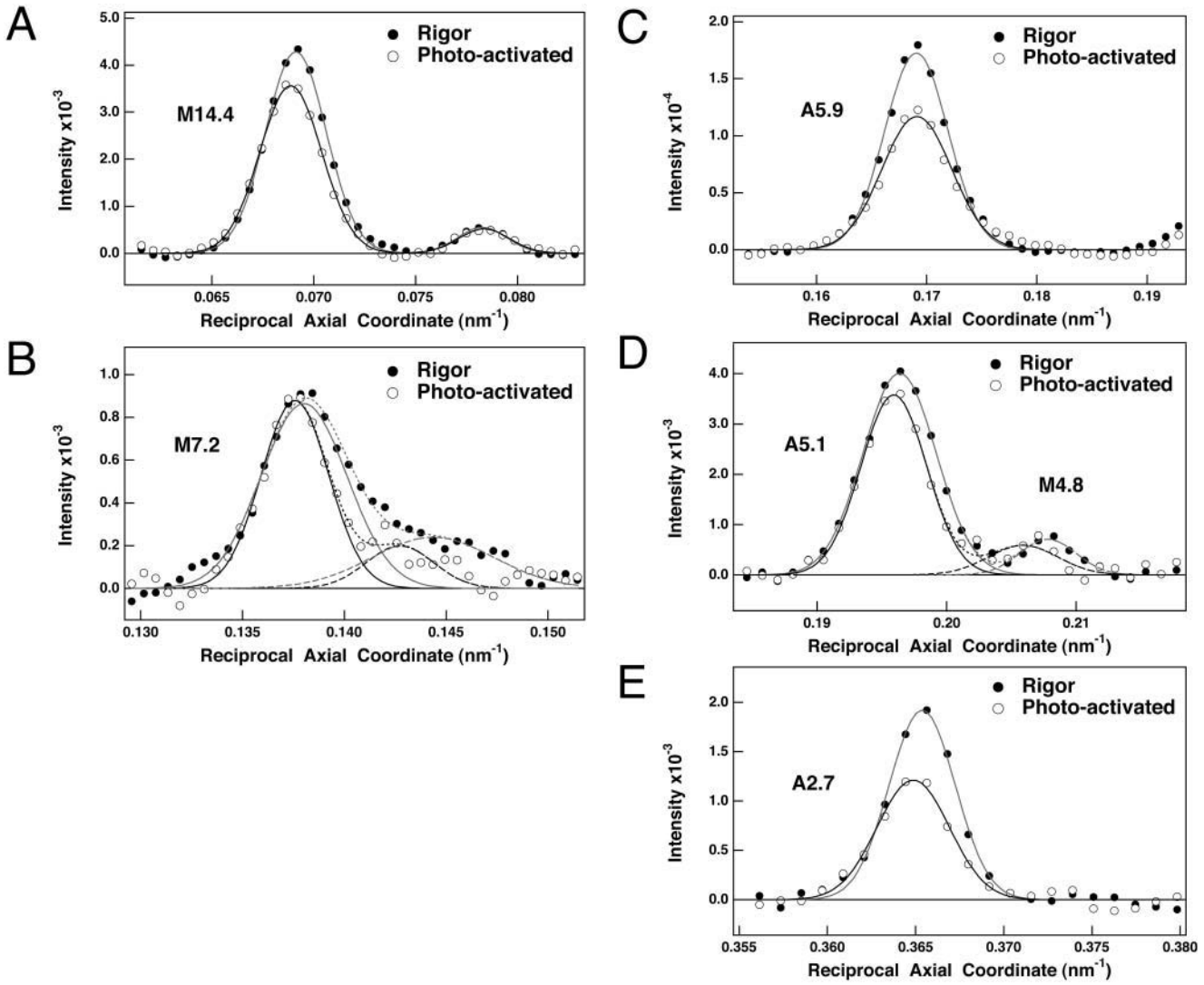

FIGURE 4 Axial intensity profiles of characteristic x-ray reflections in the two-dimensional diffraction patterns from rigor and photoactivated muscle fibers. (*A* and *B*) The 14.4-nm and the 7.2-nm myosin-based meridional reflections, respectively; (*C* and *D*) the 5.9-nm and 5.1-nm actin-based layer lines, respectively; and (*E*) the 2.7-nm actin-based meridional reflection. (●) Rigor muscle fibers and (○) photoactivated muscle fibers.

seen that x-ray diffraction patterns of photoactivated muscle fibers are distinctly different from those of relaxed muscle fibers and of fully Ca^{2+}-activated muscle fibers. The overall appearance of the photoactivated patterns resembles the rigor patterns, but the two patterns exhibit significant differences in intensity profiles of characteristic reflections as below.

The axial intensity profiles of several reflections in the photoactivated and the rigor patterns are depicted in Fig. 4. When compared with those of the corresponding reflections in the rigor patterns, the intensities of the 14.4-nm first- and 7.2-nm second-order myosin-based meridional reflections with a 14.4-nm repeat (Fig. 4, *A* and *B*) as well as the 5.9-nm and 5.1-nm actin-based layer lines (Fig. 4, *C* and *D*) and the 2.7-nm actin-based meridional reflection (Fig. 4 *E*) were significantly weaker in the photoactivated patterns. The 21.5-nm myosin-based ''forbidden'' meridional reflection became markedly weaker by the photoactivation (data not shown). The axial centroids of the myosin- and actin-based reflections in the photoactivated pattern shifted toward the low-angle side showing an increase in the axial spacing, although that of the 5.9-nm layer line stayed mostly at the same position. Fig. 5 summarizes as histograms the axial spacing of myosin-based (*A*) and actin-based (*B*) reflections in rigor, photoactivated, and fully Ca^{2+}-activated patterns relative to those of the corresponding reflections in the relaxed pattern. It should be noted that, when muscle fibers in the rigor state were fully activated, the axial spacings of the myosin-based and actin-based reflections similarly increased except that of the 5.9-nm layer line.

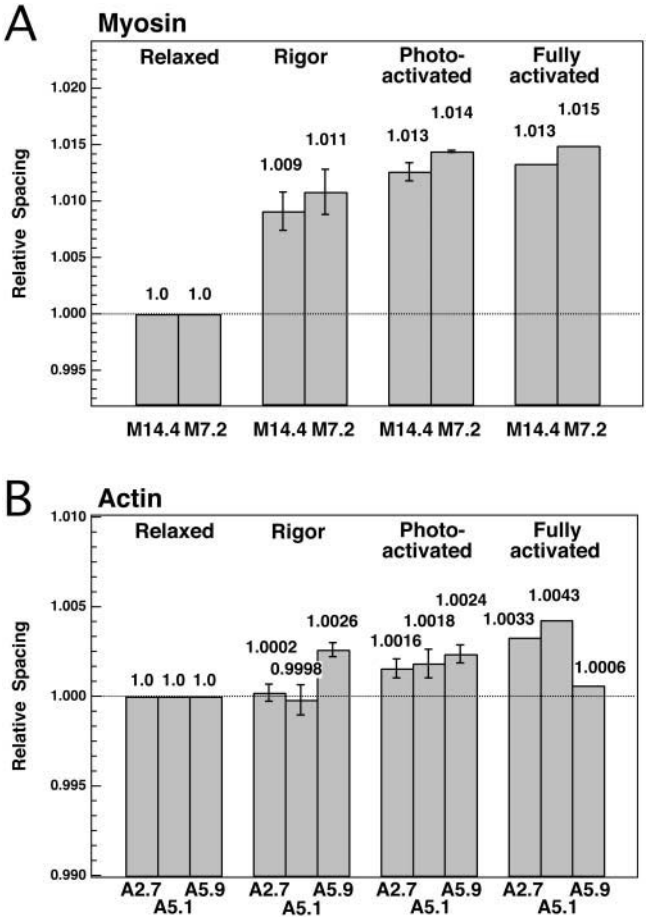

FIGURE 5 Histograms of the axial spacings of characteristic myosin-based reflections (*A*) and actin-based reflections (*B*) from photoactivated, rigor, and fully activated muscle fibers relative to those of the corresponding reflections from relaxed muscle fibers. In *A*, M14.4 and M7.2 denote the 14.4-nm and 7.2-nm myosin-based meridional reflections, and in *B*, A2.7, A5.1, and A5.9, the 2.7-nm actin-based meridional and the 5.1-nm and 5.9-nm actin-based layer-line reflections. In *A* and *B*, the number on each bar graph denotes the average value for the relative spacing, and the vertical line is a standard error of the mean ($n = 4$). Any differences in the bar graph are statistically significant in the transition from the rigor state to the photoactivated state. The axial spacings of reflections from fully Ca^{2+}-activated muscle fibers were obtained only from one data set.

Fig. 6 compares the radial intensity profiles of several reflections in the photoactivated and rigor patterns. The integrated intensity of the 14.4-nm meridional reflection from photoactivated muscle fibers decreased by ~11% with a concomitant increase of ~15% in radial width (Fig. 6 *A*). The integrated intensity of the 7.2-nm reflection decreased by ~14% without an appreciable change of the radial width (Fig. 6 *B*). On the other hand, the overall intensity of the 36.7-nm actin-based first layer line in the photoactivated patterns substantially decreased with a more marked drop at the inner peak near the meridian (Fig. 6 *C*). Similarly the intensity of the 5.9-nm layer line decreased to a greater extent on its small-angle side ($0.01 < R < 0.07$ nm^{-1}) retaining an additional broad shoulder on the large-angle side of the profile characteristic of the rigor pattern (Fig. 6 *D*). In contrast, the intensity decrease of the 5.1-nm layer line in the photoactivated pattern was relatively small (Fig. 6 *E*). The intensity of the 2.7-nm meridional reflection decreased by ~30% (see Fig. 4 *E*). The integrated intensities of these reflections from photoactivated and relaxed muscle fibers relative to those of the corresponding reflections from rigor muscle fibers are summarized in Table 2.

Unfortunately, limitations of the present techniques made it difficult to measure time-dependent changes of the two-dimensional x-ray diffraction patterns from small muscle fiber bundles with an adequate time-resolution.

Electron microscopic images of photoactivated muscle fibers

Fig. 7 shows typical electron micrographs of rigor muscle fibers (*A*) and photoactivated muscle fibers (*B*) for thin sections cut along the (110) lattice plane of the hexagonal myofilament array. The images of the electron micrographs of photoactivated fibers, obtained by freezing at 1.9 s after the photoactivation, were very similar to those of rigor muscle fibers, although distinct differences could be seen between the two images. For photoactivated muscle fibers, the 36.7-nm crossover repeat of two long-pitched helical strands in the actin filament was less obvious and the thin filaments had a more zigzag appearance. The optical diffraction patterns of these electron micrographs as shown at the bottom of each micrograph in Fig. 7 revealed that the intensity of the 14.4-nm reflection due to the myosin cross-bridge repeat for photoactivated muscle fibers was slightly weaker and broader when compared with that for original rigor muscle fibers. These results are consistent with the intensity changes of the corresponding x-ray reflection from photoactivated muscle fibers as mentioned above.

The cross-bridge angles to the thick filaments in these electron micrographs were determined by the computer-assisted analysis after the images of cross-bridges and myofilaments were converted to the short-rod images (see Materials and Methods). The distributions of the cross-bridge angles to the thick filaments thus obtained for rigor and photoactivated muscle fibers are depicted as histograms in Fig. 8. Although in both muscle fibers the cross-bridges were broadly distributed over the orientation angle of 60–110°, the cross-bridge angles in rigor fibers were centered at ~90° and relatively narrowly distributed in a symmetric fashion. In photoactivated muscle fibers, they were centered at ~85° and more widely distributed in an asymmetric fashion with more in the small angle side. Thus during the photoactivation, the cross-bridge orientation changed from nearly perpendicular to the thick filaments to both sides of ~85° with more in the direction of force generation.

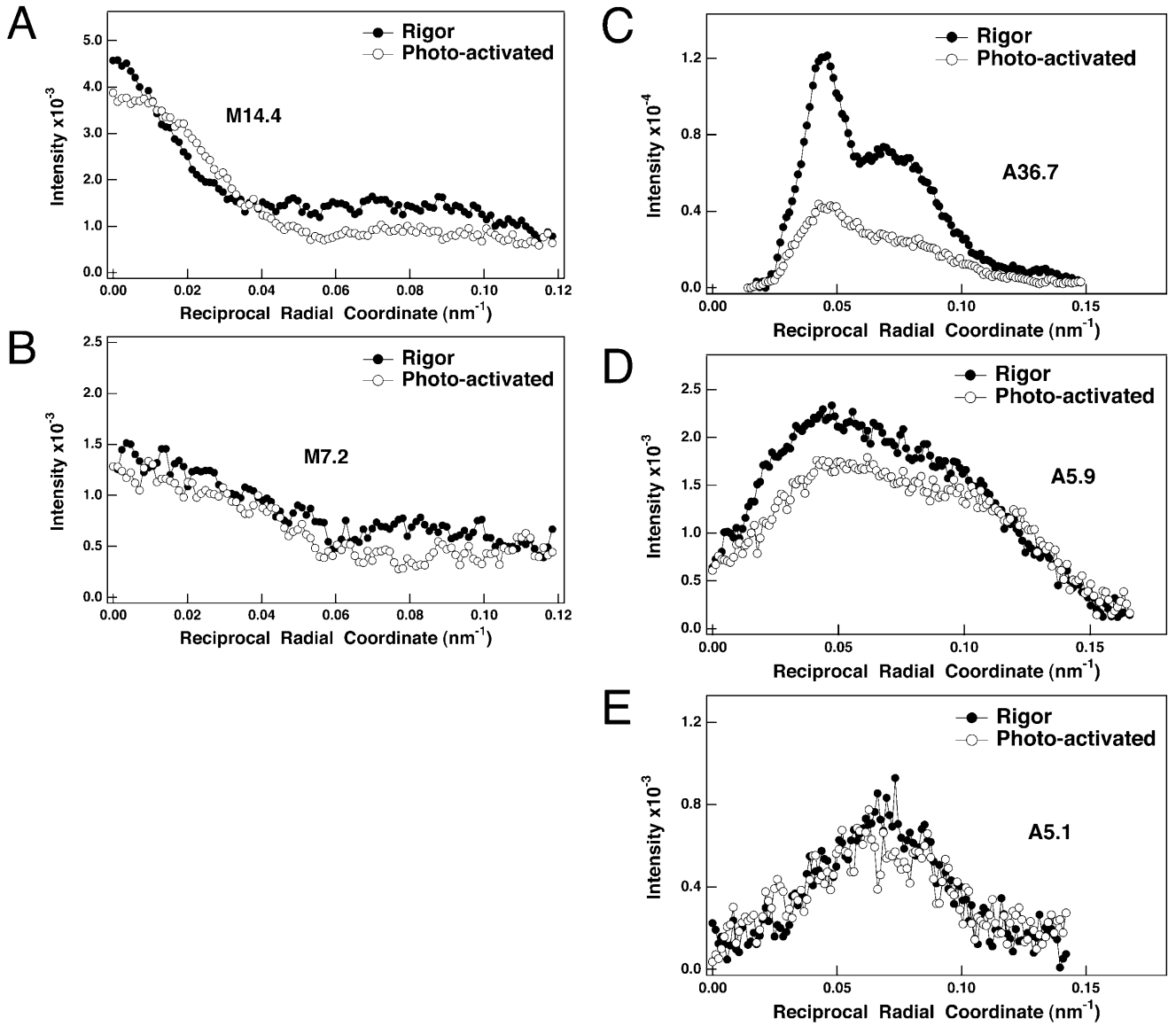

FIGURE 6 Radial intensity profiles of characteristic x-ray reflections from rigor and photoactivated muscle fibers. (*A* and *B*) The 14.4-nm, and 7.2-nm myosin-based meridional reflections, respectively, and (*C–E*) the 36.7-nm, 5.9-nm, and 5.1-nm actin-based layer-line reflections, respectively. (●) Rigor muscle fibers and (○) photoactivated muscle fibers.

DISCUSSION

Rigor force production in photoactivated muscle fibers

In the present studies, a substoichiometric amount of ATP (~100 μM) was photogenerated in the presence of Ca^{2+} in isometric muscle fibers initially in the rigor state. After the photogeneration of ATP, isometric muscle fibers transiently showed a slight decrease in the force level and then produced a long lasting rigor force whereas their stiffness slightly decreased and quickly returned to that of the initial rigor level almost in parallel to the development of force (Fig. 1).

In rigor muscle fibers before the photoactivation, all myosin heads in a muscle fiber are attached to actin filaments (Cooke and Franks, 1980; Lovell et al., 1981). When a substoichiometric amount of ATP is photogenerated, a limited population of the myosin heads in muscle fibers hydrolyzes ATP based on the acto-myosin ATPase scheme (Geeves et al., 1984) whereas other myosin heads with no available ATP to bind remain attached to the actin filaments. As ATP has high affinity to myosin heads, we may assume that almost all photogenerated ATP molecules quickly bind to the myosin heads (M) attached to the actin filaments (A) forming an AM.ATP complex. Thus in photoactivated muscle fibers, ~67% of the myosin heads would bind

TABLE 2 Integrated intensities for the characteristic x-ray reflections from photoactivated, relaxed, and fully Ca^{2+}-activated muscle fibers relative to those for the corresponding reflections from rigor muscle fibers

	Relative intensities		
Reflections	Photoactivated	Relaxed	Fully activated
36.7 (nm) (A)	−59 (%)	−91 (%)	N.D.
14.4* (M)	−11	+10	−32
7.2* (M)	−14	+70	+20
7.1 (A)	−31	N.D.	N.D.
5.9 (A)	−17	−52	−30
5.1 (A)	−8	−38	−42
2.7* (A)	−31	−90	−44

N.D., not determined.
*Meridional reflection; (A), actin-based reflection; and (M), myosin-based reflection.

a photogenerated ATP and ~33% of the myosin heads will bind no ATP. Then the ATP-bound myosin heads detach from or weakly bind to the actin filaments by changing their conformation to isomerize into an AM*·ATP complex (a symbol on M represents an altered conformation of myosin). After the transition from the AM*·ATP state to an AM**·ADP·Pi state (Pi represents a product inorganic phosphate) with a further alteration of their conformation, the myosin heads transform to strongly bind to the actin filaments. Then in association with the transition from the AM**·ADP·Pi state to an AM^{+}·ADP + Pi state, the binding of the myosin heads become strong and the contractile force is thought to be produced. Finally the product ADP is released from the myosin heads. As no further ATP is available, the myosin heads initially bound photogenerated ATP will complete one ATPase cycle and stop at the end of this cycle with attached to the actin filaments.

Thus in photoactivated muscle fibers, the ATP-bound cross-bridges will transiently detach from the actin filaments and quickly reattach to the actin filaments whereas a significant population of the cross-bridges with no ATP to bind will remain attached to the actin filaments. The former cross-bridges will produce an active force and, at the end of the ATP hydrolysis cycle, could sustain the produced force as a passive rigor force whereas the latter cross-bridges will not contribute to generate the rigor force. The above experimental results of force and stiffness changes associated with the photoactivation of rigor muscle fibers are consistent with an ATP hydrolysis process mentioned above.

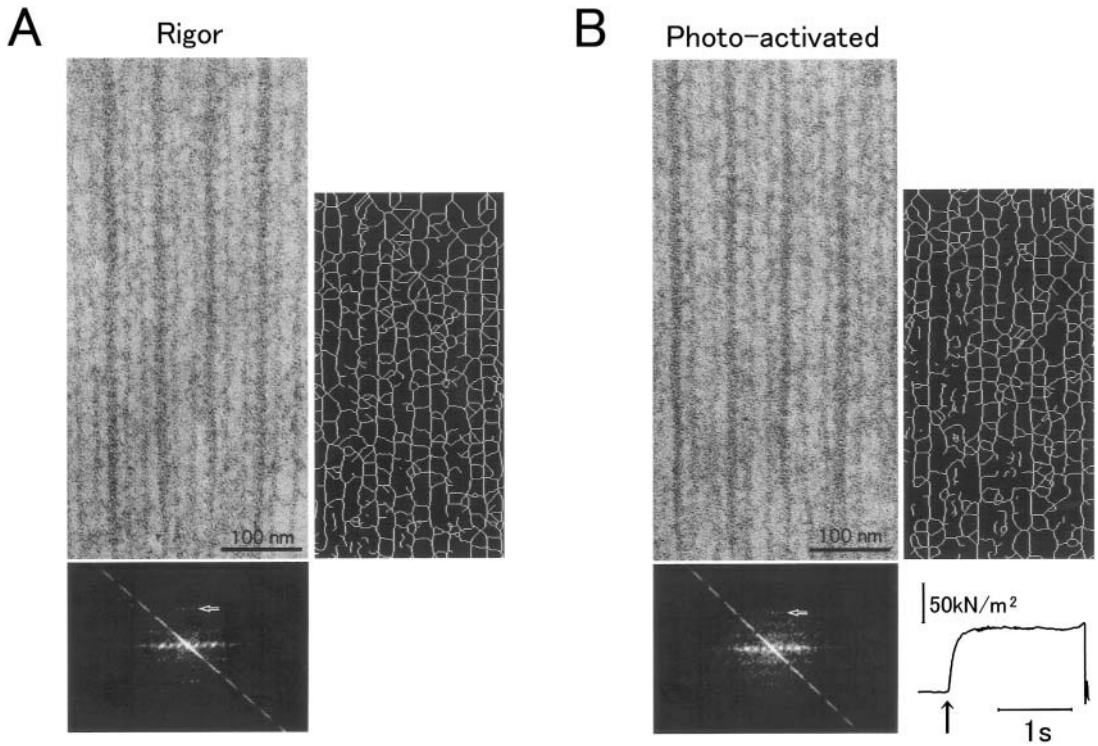

FIGURE 7 Electron micrographs of rigor and photoactivated muscle fibers sliced along the (110) lattice plane of the hexagonal myofilament array. (*A*) Rigor muscle fibers before the photoactivation, and (*B*) photoactivated muscle fibers. Below each electron micrograph is the optical diffraction pattern in which the arrow indicates the reflection corresponding to the 14.4-nm cross-bridge repeat. At the right-hand side is the short-rod images of the cross-bridges and myofilaments drawn by the computer-assisted processing. At the right-hand side of the bottom of *B* is the force trace of photoactivated muscle fibers during the freezing procedure. At the arrow, the muscle preparation was irradiated with a light flash to generate ATP, and at the end of the trace were artifact force signals produced by dipping the muscle preparation into liquid N_2.

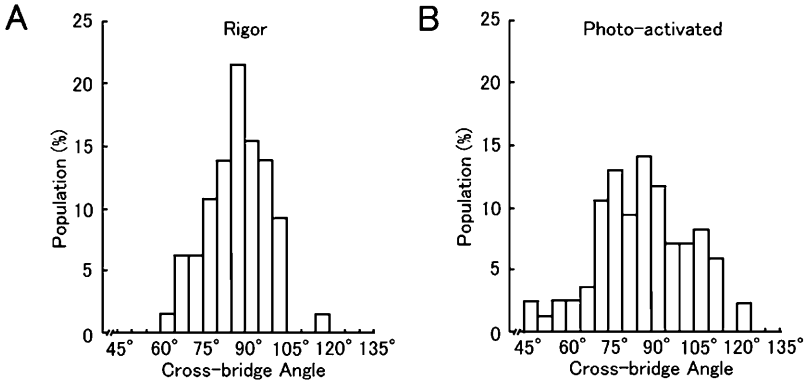

FIGURE 8 Distributions of the cross-bridge angles to the thick filament axis in the electron micrographs of sectioned rigor and photoactivated muscle fibers. (*A*) Rigor muscle fibers before the photoactivation ($n = 115$), and (*B*) photoactivated muscle fibers 1.9 s after the photoactivation ($n = 139$).

Cross-bridge configurations for the rigor force production in photoactivated muscle fibers

As shown in Results, the equatorial x-ray diffraction pattern from muscle fibers changed in association with the photoactivation and the changes lasted over seconds. Consistent with this observation, two-dimensional x-ray diffraction patterns and quick-freeze electron micrograph images obtained from muscle fibers 1–2 s after the photoactivation were different from those of initial rigor fibers. These results clearly indicate that the cross-bridge configuration(s) producing the rigor force are different from those in original rigor muscle fibers.

In equatorial x-ray diffraction patterns from photoactivated muscle fibers, the intensities of the 1,0 and 1,1 reflections changed in a reciprocal manner (Fig. 2 *A*): a very rapid fall in the 1,1 intensity and a rapid increase in the 1,0 intensity. These intensity changes were followed by a much slower return that paralleled the decline of rigor force (Fig. 2 *B*). The fast initial x-ray intensity changes indicate the rapid movements of cross-bridge mass away from the thin filaments, corresponding to the ATP-induced cross-bridge detachment. The intensity changes almost fully completed within the rapid initial phase, implying that the detached myosin heads stayed close to the thin filaments and quickly rearranged to reattach to the nearest actin monomers. This result suggests that the thin filaments were fully switched on, consistent with the situation that the initial rigor cross-bridges with no bound ATP were distributed randomly along the thin filaments. Although the magnitude of these equatorial reflection changes produced for the present photoactivated fibers was much smaller than that produced when muscle fibers were fully activated by the photolysis of caged ATP (Poole et al., 1991), these results suggest that, in photoactivated muscle fibers, the configurations of immediately reattached myosin heads rearranged on the thin filaments to produce the rigor force in a similar fashion as those taking place in fully activated muscle fibers to produce active force (Malinchik and Yu, 1995).

In two-dimensional x-ray diffraction patterns from photoactivated muscle fibers, the intensities of the 14.4-nm myosin-based meridional reflections became weaker by 10–15% (Fig. 4, *A* and *B*, and Fig. 6, *A* and *B*). The decrease in the integrated intensity of the 14.4-nm myosin-based reflections means that a cross-bridge mass projected onto the filament axis became more extended. The increase in the radial width of the 14.4-nm reflection, which was also found to take place substantially during active force generation, is caused by a change in the sampling effect as a consequence of some axial disordering of the cross-bridges along the thick filaments, although it does not affect the 7.2-nm reflection width. The so-called forbidden 21.5-nm myosin meridional reflection became markedly weaker. Similar x-ray intensity reduction in these reflections was observed in fully contracting muscle fibers and explained as the variation of each cross-bridge repeat within the 43-nm period of the thick filaments was reduced and the myosin cross-bridges changed their structures projected onto the filament axis (Yagi et al., 1981; Oshima et al., 2003). The intensities of the actin-based reflections also decreased markedly (Fig. 4, *C–E*, Fig. 6, *C–E*, and Table 2). The intensities of the 5.9-nm and 36.7-nm layer lines decreased to a greater extent near the meridian, in which the large intensity drop in the latter layer line could partly be caused by the changes in the lattice sampling effect. The inner intensity reduction of these reflections is attributed to the rearrangement of myosin heads with different configurations.

Furthermore the axial spacings of both the actin-based reflections (5.9 nm, 5.1 nm, and 2.7 nm) and the myosin-based meridional reflections (14.4 nm and 7.2 nm) increased by the photoactivation (Figs. 4 and 5), indicating that the thick myosin and the thin actin filaments extended in association with the rigor force production as in muscle fibers during the active force development (Huxley et al., 1994; Wakabayashi et al., 1994; Takezawa et al., 1998). A very small change in the 5.9-nm reflection spacing in photoactivated fibers indicates that the actin filaments extended accompanied with a twisting of their helical structure as in fully activated muscle fibers (Wakabayashi et al., 1994; Takezawa et al., 1998; Bordas et al., 1999). These axial spacing changes of the myosin-based as well as the actin-

based reflections contain characteristics of the actively contracting muscle fibers.

Thus two-dimensional x-ray diffraction patterns from photoactivated muscle fibers resembled the initial rigor patterns but contained some diffraction features characteristic of actively contracting muscle fibers. These x-ray results clearly indicate that a significant population of the cross-bridges in photoactivated muscle fibers first turns to active force generation configuration(s) to produce the force as in fully activated muscle fibers and then sustained the produced force as a passive rigor force by being locked in a configuration(s) having characteristics of active force-generating configuration(s).

Comparable myosin-based x-ray diffraction changes were observed for actively contracting muscle fibers, and the observed changes have quantitatively been explained by the computer simulation assuming that, after the reattachment to actin filaments, the cross-bridges change their configuration or the myosin heads make segmental rearrangements over the actin filaments toward the direction of force generation (Irving et al., 1992; Yagi et al., 1996; Diaz Banos et al., 1996; Takezawa et al., 1999; Linari et al., 2000; Iwamoto et al., 2001). Thus we may assume that, in photoactivated muscle fibers, the rigor force was sustained in a similar fashion by the reattached cross-bridges oriented relative to thin filaments in the force-generating direction, possibly by bending the light chain binding domain of the myosin heads. This assumption is in accordance with the cross-bridge angle changes observed in the electron micrographs of photoactivated muscle fibers (Fig. 8).

The present results for photoactivated muscle fibers can be contrasted with the changes in the x-ray diffraction patterns produced by stretching rigor muscle fibers (Tanaka et al., 1991; Yagi et al., 1996; Dobbie et al., 1998; Takezawa et al., 1999) and by the addition of MgADP to rigor fibers (Takezawa et al., 1999). In both of these cases the intensities of the 14.4 nm-based meridional reflections increased, indicating that cross-bridges turned toward a more perpendicular orientation to the thin filaments, opposite to the direction of the cross-bridge orientation in photoactivated fibers. These observations suggest that the cross-bridge configuration(s) producing the rigor force cannot be transformed from the rigor configuration(s) by simply stretching rigor fibers or adding MgADP to rigor muscle fibers.

In photoactivated muscle fibers, the produced rigor force declined in parallel with the recovery of the 1,1 equatorial x-ray intensity with a time constant of 4 s. The rate of these changes is much faster than that of the force decline induced after stretching rigor muscle fibers (Somasundaram et al., 1989) and it is rather comparable in magnitude to the breaking rate of the actomyosin bonds (Nishizaka et al., 2000). This suggests that the cross-bridges producing the rigor force are attached to actin filaments not in the rigor configuration but in an unstable and strained configuration(s), and subject to rearrangement over actin filaments to the rigor configuration(s) by nullifying the produced strain.

Cross-bridge rearrangements to produce the rigor force in photoactivated muscle fibers

During rigor force development in photoactivated muscle fibers, the detached heads actively reattach and burn up ATP asynchronously rearranging their configuration(s), and they will end up distributed over different angles attached to the thin actin filaments, producing a net positive force due to the different steric constraints the individual heads have depending on the history of their neighbors. We will analyze how the cross-bridges rearrange to produce the rigor force in photoactivated muscle fibers by simplifying the cross-bridge configurations involved.

First we estimate the population of the cross-bridges attached to the actin filaments in a rigor configuration in photoactivated muscle fibers. It is assumed that neglecting a possible contribution from regulatory proteins the actin-based x-ray reflections from rigor muscle fibers have contributions from the actin filaments themselves and an additional contribution from the myosin heads attached to the actin filaments in the rigor configuration. In this assumption the x-ray intensity of the actin-based reflections is proportional to $|\mathbf{F_A} + 0.6q\mathbf{F_M}|^2$, where $\mathbf{F_A}$ and $\mathbf{F_M}$, respectively, denote the x-ray structure factors of the actin monomer in the filament and of the myosin head attached to the actin filaments in the rigor configuration, and q the fraction of myosin heads attached to the actin filaments in the rigor configuration (Squire, 1981; Kim et al., 1998). The factor of 0.6 in the above equation corresponds to the population of the actin sites occupied by the myosin heads in rigor muscle fibers. The value for $|\mathbf{F_A}|$ was derived based on the integrated intensities of the actin-based reflections of relaxed muscle fibers by assuming that all the myosin heads are detached from the actin filaments (i.e., $q = 0$). The value for $|\mathbf{F_M}|$ was derived based on the integrated intensities of the actin-based reflections of rigor muscle fibers by assuming that all the myosin heads attach to the actin filaments with the rigor configuration (i.e., $q = 1.0$). It should be noted that the magnitude of $|\mathbf{F_M}|^2$ is likely less than that derived from the

TABLE 3 Fraction (q) of the myosin-heads attached to actin filaments with the rigor configuration in photoactivated muscle fibers estimated from the integrated intensities of the characteristic actin-based x-ray reflections in Table 2

Reflections	Fraction (q)
36.7 (nm)	0.46
7.1	0.77
5.9	0.77
5.1	0.85
2.7	0.75
	(0.72)

The number in parentheses denotes the average value.

integrated x-ray intensities from the actin filaments fully decorated with isolated myosin heads because the steric constraints produced in the myofilament lattice could alter the configurations of myosin heads attached to the actin filaments (Arata, 1990; Hirose et al., 1993; Lenart et al., 1996; and Fig. 8). Assuming that $|\mathbf{F_A}|$ and $|\mathbf{F_M}|$ are proportional to the molecular weight of the respective molecules, we analyzed several actin-based x-ray intensities of photoactivated muscle fibers to obtain their q value. The q values for different reflections are listed in Table 3. The small q value from the 36.7-nm intensity might be due partly to an intensity drop caused by nonuniform movements of the myofilaments in association with the force development as mentioned above. The averaged q value is 0.72. Thus the fraction of the myosin heads attached to the actin filaments in the rigor configuration in photoactivated muscle fibers is estimated to be ~70%, which is substantially greater than the population of the myosin heads not photoactivated and expected to remain attached to the actin filaments in the rigor configuration (~33%). The above analysis suggests that roughly a half of photoactivated myosin heads returned to the rigor configuration(s) shortly after the photoactivation.

Second, we briefly consider how cross-bridges rearrange to produce the rigor force in photoactivated muscle fibers. As the myofilaments cannot slide very far in photoactivated muscle fibers because of the residual original rigor heads (Yamada et al., 1993), a detached head would reattach to either the actin monomer to which it was originally attached or an actin monomer displaced one or two monomers away in either direction. It is reasonable to assume that the former myosin heads will not contribute to produce a net rigor force if they simply return to the original rigor configurations. Considering the above analysis, the population of such myosin heads would be about a half of the photoactivated myosin heads. On the other hand, the latter myosin heads will adopt a configuration different from the original rigor configuration and produce the active force by going through the active configuration(s). After the ATPase reaction is completed, they could sustain the produced rigor force by being locked in a passive noncycling state(s). The myosin heads reattached to the actin monomers located toward the Z-line and M-line away from the original partner actin monomers will produce either positive or negative forces (Dantzig et al., 1991), the magnigude of which would change due to neighboring attached heads. In photoactivated muscle fibers, a positive rigor force was produced under isometric conditions, and under unloaded conditions, photoactivated muscle fibers shortened, not lengthened (Yamada et al., 1993), suggesting that a majority of detached heads preferentially reattached to the adjacent actin monomers located toward the Z-line direction and oriented toward the force generation direction. As these heads have configuration(s) different from the original rigor configuration(s), they will be subject to structural distortions or constraints to induce the relaxation of rigor force.

In conclusion, the present studies indicate that the rigor force is produced when the detached cross-bridges first reattach to thin filaments in the active force-generating state(s) and then transform to a stable noncycling state(s). They are tilted over the thin actin filaments having some characteristics of the active force-generating configuration(s). The cross-bridges producing the rigor force are in a quasi-stable force-sustaining configuration(s) transformable via the actively force-generating configuration(s) but not via the rigor configuration(s).

The authors express their hearty thanks to professor H. Sugi, Teikyo University, for his support and encouragement. They also thank Dr. Y. Amemiya, The University of Tokyo, for his technical support for x-ray diffraction experiments at the Photon Factory, KEK. They appreciate Dr. R. Shibayama, Teikyo University, for her assistance on electron microscopic analysis, and Dr. Y. Kunioka, Tokyo University of Science, for her assistance on the artwork.

This work was approved by the Photon Factory Advisory Committee.

REFERENCES

Allen, T. S., N. Ling, M. Irving, and Y. E. Goldman. 1996. Orientation changes in myosin regulatory light chains following photorelease of ATP in skinned muscle fibers. *Biophys. J.* 70:1847–1862.

Arata, T. 1990. Orientation of spin-labeled light chain 2 of myosin head in muscle fibers. *J. Mol. Biol.* 214:471–478.

Bordas, J., A. Svensson, M. Rothery, J. Lowy, G. P. Diakun, and P. Boesecke. 1999. Extensibility and symmetry of actin filaments in contracting muscles. *Biophys. J.* 77:3197–3207.

Cooke, R. 1997. Actomyosin interaction in striated muscle. *Physiol. Rev.* 77:671–697.

Cooke, R., and K. Franks. 1980. All myosin heads form bonds with actin in rigor rabbit skeletal muscle. *Biochemistry.* 19:2265–2269.

Corrie, J. E. T., B. D. Brandmeier, R. E. Ferguson, D. R. Trentham, J. Kendrick-Jones, S. C. Hopkins, U. A. van der Heide, Y. E. Goldman, C. Sabid-Davis, R. E. Dale, S. Criddle, and M. Irving. 1999. Dynamic measurement of myosin light-chain-domain tilt and twist in muscle contraction. *Nature (Lond.).* 400:425–430.

Dantzig, J. A., M. G. Hibberd, D. R. Trentham, and Y. E. Goldman. 1991. Cross-bridge kinetics in the presence of MgADP investigated by photolysis of caged ATP in rabbit psoas muscle fibres. *J. Physiol.* 432:639–680.

Diaz Banos, F. G., J. Bordas, J. Lowy, and A. Svensson. 1996. Small segmental rearrangements in the myosin head can explain force generation in muscle. *Biophys. J.* 71:576–589.

Dobbie, I., M. Linari, G. Piazzesi, M. Reconditi, N. Koubassova, M. A. Ferenczi, V. Lombardi, and M. Irving. 1998. Elastic bending and active tilting of myosin heads during muscle contraction. *Nature.* 396:383–387.

Ferenczi, M. A., E. Homsher, and D. R. Trentham. 1984. The kinetics of magnesium adenosine triphosphate cleavage in skinned muscle fibres of the rabbit. *J. Physiol.* 352:575–599.

Fisher, A. J., C. A. Smith, J. Thoden, R. Smith, K. Sutoh, H. M. Holden, and I. Rayment. 1995. Structural studies of myosin:nucleotide complexes: a revised model for the molecular basis of muscle contraction. *Biophys. J.* 68:19S–26S.

Geeves, M. A., R. S. Goody, and H. Gutfreund. 1984. Kinetics of acto-S-1 interactions as a guide to a model for the crossbridge cycle. *J. Muscle Res. Cell Motil.* 5:351–361.

Highsmith, S., and D. Eden. 1993. Myosin-ATP chemomechanics. *Biochemistry.* 32:2455–2458.

Hirose, K., T. D. Lenart, J. M. Murray, C. Franzini-Armstrong, and Y. E. Goldman. 1993. Flash and smash: rapid freezing of muscle fibers activated by photolysis of caged ATP. *Biophys. J.* 65:397–408.

Houdusse, A., A. G. Szent-Gyorgyi, and C. Cohen. 2000. Three conformational states of scallop myosin S1. *Proc. Natl. Acad. Sci. USA.* 97:11238–11243.

Huxley, H. E. 1969. The mechanism of muscular contraction. *Science.* 164:1356–1366.

Huxley, H. E., A. Stewart, H. Sosa, and T. C. Irving. 1994. X-ray diffraction measurements of the extensibility of actin and myosin filaments in contracting muscle. *Biophys. J.* 67:2411–2421.

Irving, M., V. Lombardi, G. Piazzesi, and M. A. Ferenczi. 1992. Myosin head movements are synchronous with the elementary force-generating process in muscle. *Nature (Lond.).* 357:156–158.

Iwamoto, H., K. Oiwa, T. Suzuki, and T. Fujisawa. 2001. X-ray diffraction evidence for the lack of stereospecific protein interaction in highly activated actomyosin complex. *J. Mol. Biol.* 305:863–874.

Kabsch, W., H. G. Mannherz, D. Suck, E. F. Pai, and K. C. Holmes. 1990. Atomic structure of the acin:DNase I complex. *Nature (Lond.).* 347: 37–44.

Katayama, E. 1998. Quick-freeze deep-etch electron microscopy of the actin-heavy meromyosin complex during the in vitro motility assay. *J. Mol. Biol.* 278:349–367.

Kawai, M., and P. W. Brandt. 1976. Two rigor states in skinned crayfish single muscle fibers. *J. Gen. Physiol.* 68:267–280.

Kim, D.-S., Y. Takezawa, M. Ogino, T. Kobayashi, T. Arata, and K. Wakabayashi. 1998. X-ray diffraction studies on the structural changes of rigor muscles induced by binding of phosphate analogs in the presence of MgADP. *Biophys. Chem.* 74:71–82.

Lenart, T. D., J. M. Murray, C. Franzini-Armstrong, and Y. E. Goldman. 1996. Structure and periodicities of crossbridges in relaxation, in rigor, and during contractions initiated by photolysis of caged Ca^{2+}. *Biophys. J.* 71:2289–2306.

Linari, M., L. Lucii, M. Reconditi, M. E. Vannicelli Casoni, H. Amenitsch, S. Bernstorff, G. Piazzesi, and V. Lombardi. 2000. A combined mechanical and x-ray diffraction study of stretch potentiation in single frog muscle fibres. *J. Physiol.* 526.3:589–596.

Lovell, S. J., P. J. Knight, and W. F. Harrington. 1981. Fraction of myosin heads bound to thin filaments in rigor filaments from insect flight and vertebrate muscles. *Nature (Lond.).* 293:664–666.

Malinchik, S., and Y. C. Yu. 1995. Analysis of equatorial x-ray diffraction patterns from muscle fibers: factors that affect the intensities. *Biophys. J.* 68:2023–2031.

Mendelson, R., D. Schneider, and D. Stone. 1996. Conformations of myosin subfragment-1 ATPase intermediates from neutron and x-ray scattering. *J. Mol. Biol.* 256:1–7.

Nishizaka, T., R. Seo, H. Tadakuma, K. Kinosita, and S. Ishiwata. 2000. Characterization of single actomyosin rigor bonds: load dependence of lifetime and mechanical properties. *Biophys. J.* 79:962–974.

Oshima, K., Y. Takezawa, Y. Sugimoto, M. Kiyotoshi, and K. Wakabayashi. 2003. Modeling analysis of myosin-based meridional x-ray reflections from frog skeletal muscles in relaxed and contracting states. *Adv. Exp. Med. Biol.* In press.

Poole, K. J. V., Y. Maeda, G. Rapp, and R. S. Goody. 1991. Dynamic x-ray diffraction measurements following photolytic relaxation and activation of skinned rabbit psoas fibres. *Adv. Biophys.* 27:63–75.

Rayment, I., W. R. Rypniewski, K. Schmidt-Base, R. Smith, D. R. Tomchick, M. M. Benning, D. A. Winkelmann, G. Wesenberg, and H. M. Holden. 1993a. Three-dimensional structure of myosin subfragment-1: a molecular motor. *Science.* 261:50–58.

Rayment, I., H. M. Holden, M. Whittaker, C. B. Yohn, M. Lorenz, K. C. Holmes, and R. A. Milligan. 1993b. Structure of the actin-myosin complex and its implications for muscle contraction. *Science.* 261:58–65.

Shih, W. M., Z. Gryczynski, J. R. Lakowicz, and J. A. Spudich. 2000. A FRET-based sensor reveals large ATP hydrolysis-induced conformational changes and three distinct states of the molecular motor myosin. *Cell.* 102:683–694.

Somasundaram, B., A. Newport, and R. T. Tregear. 1989. Slip of rabbit striated muscle in rigor or AMPPNP. *J. Muscle Res. Cell Motil.* 10:360–368.

Squire, J. 1981. The Structural Basis of Muscular Contraction. Plenum Press, New York, Chap. 7.

Sugimoto, Y., M. Tokunaga, Y. Takezawa, M. Ikebe, and K. Wakabayashi. 1995. Conformational changes of the myosin heads during hydrolysis of ATP as analyzed by x-ray solution scattering. *Biophys. J.* 68:29S–34S.

Suzuki, S., and H. Sugi. 1983. Extensibility of the myofilaments in vertebrate skeletal muscle as revealed by stretching rigor muscle fibers. *J. Gen. Physiol.* 81:531–546.

Suzuki, S., Y. Oshimi, and H. Sugi. 1993. Freeze-fracture studies on the cross-bridge angle distribution at various states and the thin filament stiffness in single skinned frog muscle fibers. *J. Electron Microsc.* 42: 107–116.

Suzuki, Y., T. Yasunaga, R. Ohkura, T. Wakabayashi, and K. Sutoh. 1998. Swing of lever-arm of myosin motor at the isomerization and phosphate-release steps. *Nature (Lond.).* 396:380–383.

Takezawa, Y., D.-S. Kim, M. Ogino, Y. Sugimoto, T. Kobayashi, T. Arata, and K. Wakabayashi. 1999. Backward movements of cross-bridges by application of stretch and by binding of MgADP to skeletal muscle fibers in the rigor state as studied by x-ray diffraction. *Biophys. J.* 76:1770–1783.

Takezawa, Y., Y. Sugimoto, and K. Wakabayashi. 1998. Extensibility of the actin and myosin filaments in various states of skeletal muscle as studied by x-ray diffraction. *Adv. Exp. Med. Biol.* 453:309–317.

Tanaka, H., K. Wakabayashi, and Y. Amemiya. 1991. Changes in the x-ray diffraction pattern from rigor muscles by application of external length changes. *Adv. Biophys.* 27:105–114.

Taylor, K. A., H. Schmitz, M. C. Reedy, Y. E. Goldman, C. Franzini-Armstrong, H. Sasaki, R. T. Tregear, K. J. V. Poole, C. Lucaveche, R. T. Edwards, L. F. Chen, H. Winkler, and M. K. Reedy. 1999. Tomographic 3D reconstruction of quick-frozen Ca^{2+}-activated contracting insect flight muscle. *Cell.* 99:421–431.

Wakabayashi, K., and Y. Amemiya. 1991. Progress in x-ray synchrotron diffraction studies of muscle contraction. *Handbook Synchrotron Radiat.* 4:597–678.

Wakabayashi, K., Y. Sugimoto, H. Tanaka, Y. Ueno, Y. Takezawa, and Y. Amemiya. 1994. X-ray diffraction evidence for the extensibility of actin and myosin filaments during muscle contraction. *Biophys. J.* 67:2422–2435.

Wakabayashi, K., M. Tokunaga, I. Kohno, Y. Sugimoto, T. Hamanaka, Y. Takezawa, T. Wakabayashi, and Y. Amemiya. 1992. Small-angle synchrotron x-ray scattering reveals distinct shape changes of the myosin head during hydrolysis of ATP. *Science.* 258:443–447.

Yagi, N., E. J. O'Brien, and I. Matsubara. 1981. Changes of thick filament structure during contraction of frog striated muscle. *Biophys. J.* 33:121–138.

Yagi, N., K. Wakabayashi, H. Iwamoto, K. Horiuti, I. Kojima, T. C. Irving, Y. Takezawa, Y. Sugimoto, T. Majima, Y. Amemiya, and M. Ando. 1996. Small-angle x-ray diffraction of muscle using undulator radiation from the TRISTAN main ring at KEK. *J. Synchrotron Radiat.* 3:305–312.

Yamada, T., O. Abe, T. Kobayashi, and H. Sugi. 1993. Myofilament sliding per ATP molecule in rabbit muscle fibres studied using laser flash photolysis of caged ATP. *J. Physiol.* 466:229–243.

Yamada, T., H. Iwamoto, K. Wakabayashi, H. Wada, O. Abe, and H. Sugi. 1994a. Nonrigor crossbridges in single glycerinated skeletal muscle fibers produced by near stoichiometric amount of photo-released ATP. *Biophys. J.* 66:A193. (Abst.)

Yamada, T., S. Suzuki, H. Iwamoto, K. Wakabayashi, H. Wada, O. Abe, and H. Sugi. 1994b. Non-rigor crossbridges produced by near-stoichiometric amount of ATP photogenerated in glycerinated single skeletal muscle fibers. *J. Muscle Res. Cell Motil.* 15:351. (Abst.)